Preprints of the
9th International Symposium on Advanced Control of Chemical Processes
The International Federation of Automatic Control
June 7-10, 2015, Whistler, British Columbia, Canada

Graph reduction for material integrated process networks with flow segregation ⋆

Seongmin Heo and Prodromos Daoutidis

Department of Chemical Engineering and Materials Science
University of Minnesota, Minneapolis, MN 55455, USA
(email: heoxx017@umn.edu, daout001@umn.edu)

Abstract: In this paper, a scalable framework is developed to analyze complex process networks consisting of multiple material integration loops. Using information on the orders of magnitude of different material flows, the framework identifies the time scales where different process units evolve, and the manipulated inputs available in each time scale, in an automated fashion. The application of the framework is illustrated via a case study on an example process network.

Keywords: process control, graph theory, graphs, integrated plant control, networks, reduction

1. INTRODUCTION

Tight integration is the rule rather than the exception in modern chemical and energy plants. The design of integrated process networks, comprising of interconnections of reaction, separation and heat exchange units through recycle streams, provides economic benefits, however, at the expense of operational challenges. Extensive research activity has been being pursued on the analysis and control of such networks, resulting in different approaches such as passivity/dissipativity-based methods (e.g. Ydstie, 2002; Hudon and Bao, 2012), distributed control (e.g. Rawlings and Stewart, 2008; Liu et al., 2009), and quasi-decentralized control (e.g. Mhaskar et al., 2007; Sun and El-Farra, 2008).

In our previous work (Kumar and Daoutidis, 2002; Baldea et al., 2006; Jogwar et al., 2009, 2012), it has been documented that whenever integration results in large rates of recovery and recycle of material and/or energy (compared to the input/output flows) a natural time-scale hierarchy develops: individual units evolve in a fast time scale (and are affected by the large internal recycle flows) and slower network-level dynamics emerge (that are affected by the small external flows). The underlying dynamic models were shown to exhibit a singularly perturbed form, consistent with this two-time-scale behavior. A method for model reduction and hierarchical control, exploiting this time scale multiplicity, was proposed within the framework of singular perturbations.

Most industrial process networks are complex, consisting of combinations of *multiple* integration loops (instead of just one), and thus showing a potential to exhibit multiple-time-scale dynamics. The analysis of such dynamics through successive application of singular perturbations becomes cumbersome as the size of networks increases. To this end, we have developed a graph-theory based analysis framework, focusing on complex process networks with multiple *energy* integration loops (Jogwar et al., 2011; Heo et al., 2012, 2014). It mimics the singular perturbation based analysis, but is generic and scalable to large networks. However, analyzing networks with multiple *material* integration loops is more challenging, as we need to analyze the time scale properties of multiple state variables (instead of just one) of different process units simultaneously. A key to such analysis is a proper graph representation of the material flow structure of process networks.

In this paper, we first propose a novel graph formalism to represent material flows in process networks. Then, a graph-theoretic algorithm is proposed, which uses the information on the order of magnitude of the material flows in the network and their interconnectivity to automatically generate information on i) the time scales exhibited by different process variables, and ii) potential manipulated inputs acting in each time scale. We illustrate the application of the proposed framework using an example process network.

2. GRAPH-THEORETIC ANALYSIS OF COMPLEX MATERIAL INTEGRATED PROCESS NETWORKS

2.1 Graph representation of process networks

In our previous work (Jogwar et al., 2011; Heo et al., 2012), the concept of an *energy flow graph*, which captures the energy flow structure in process networks, was used as the basis for extracting the time scale properties of the energy dynamics of such networks. A direct extension of this concept to represent the material flows of process networks is to have multiple graphs that capture the flow structure of each chemical species. However, the dynamics of the holdups of different species are not independent from one another. Specifically, large flows of certain species can act as carriers of other species that exist in small quantities, thus affecting their dynamic behavior. Thus, analyzing the time scale properties of material balance variables on the basis of multiple graphs is not straightforward or even feasible.

⋆ Financial support for this work by the National Science Foundation, grant CBET-1133167, is gratefully acknowledged.

Motivated by this, we propose a new graph representation of the material flow structure in process networks. Specifically, a process network, which involves s chemical species, is represented as a *process flow graph*, which is a weighted graph $\mathcal{G}(N, E)$. In such a graph, we have:

- N: the set of nodes which can be divided into two disjoint subsets, N_n and N_a.
- N_n: the set of normal nodes which represent individual process units. There are s+1 material balance variables (s species holdups and total holdup) related to each normal node.
- N_a: the set of auxiliary nodes which represent chemical reactions.
- E: the set of edges which can be divided into two disjoint subsets, E_n and E_a.
- E_n: the set of normal edges which represent material flows.
- E_a: the set of auxiliary edges which represent the stoichiometry of chemical reactions.
- Edge weights: each edge has s weights. For a normal edge, the weights are the orders of magnitude of different chemical species flow rates. For an auxiliary edge, the weights are the stoichiometric coefficients.

To schematically distinguish the different types of nodes, normal nodes will be represented by rectangular nodes, while auxiliary nodes will be represented by circular nodes. Also, different types of edges will be distinguished schematically by representing normal edges by solid lines and auxiliary edges by dotted lines. Note that the graph-theoretic algorithm, which will be proposed later in this paper, will treat a process flow graph as an unipartite graph (i.e. a graph with one set of nodes). For a bipartite graph representation of process networks, see e.g. Friedler et al. (1992).

For a simple illustration, let us consider a continuous stirred tank reactor (CSTR) shown in Figure 1. Feed streams of A and B are fed to the reactor, where a reaction $A + B \rightarrow C + D$ occurs, to produce a product stream. This process can be represented as a process flow graph as shown in Figure 2 with the edge weights on each edge. The list of nodes is provided in Table 1.

2.2 Basic building blocks

Large material recycles are obtained when the magnitudes of the recycle flows are larger than the magnitudes of the external input/output material flows. Large material throughputs are obtained when the magnitudes of the throughput flows are larger than the magnitudes of the recycle flows. In the process flow graphs, material recycles are process flow *cycle*s (i.e. closed walks of nodes and edges such that no node, except the first node, is repeated), while material throughputs are process flow *path*s (i.e. open walks of nodes and edges, starting from a source node and terminating at a sink node such that no node is repeated).

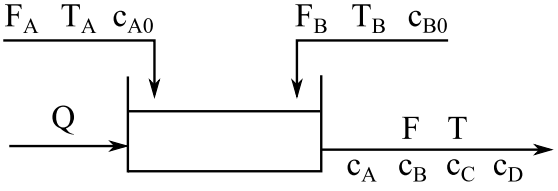

Fig. 1. A simple CSTR

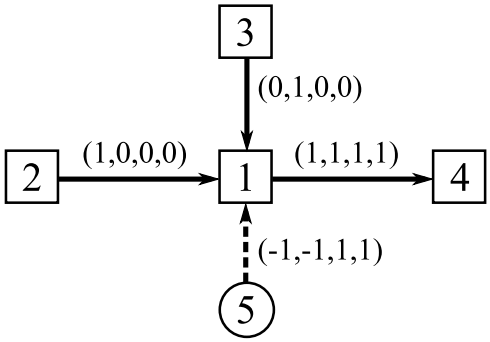

Fig. 2. Process flow graph of the simple CSTR

Normal nodes	
Node	Unit
1	CSTR
2	Feed stream source (A)
3	Feed stream source (B)
4	Product stream sink
Auxiliary nodes	
Node	Reaction
5	A+B → C+D

Table 1. Node list of the simple CSTR process flow graph

Note that it is also possible to have a combination of large material recycles and throughputs, i.e. a material flow structure can form a recycle for some chemical species and a throughput for the others. For example, in Baldea et al. (2006), process networks with recycles and purge streams were considered, and it was shown that the presence of the small purge streams induces a time scale multiplicity: the total holdup of the impurities in the recycle loop evolves in the slow time scale, while all the other variables (including the total holdup of the other chemical species in the recycle loop) evolve in the fast time scale.

The above three basic building blocks (i.e. large material recycle, large material throughput, and combination of two) can be replaced in the graph by a single composite node to reduce the complexity of the graph and to analyze the dynamics of the material balance variables in the process network. These basic building blocks will be referred to as *pure recycle*, *pure throughput*, and *partial recycle/throughput*, respectively.

Figure 3 shows a graph representation of a pure throughput over N units starting from a source supplying F_0 and ending at a sink taking F_N. Material flows of different orders of magnitude are distinguished by lines of different thickness (thick lines represent large flows, while thin lines represent smaller flows). The equivalent representation is a unit labeled $T_{L(N)}^{\mathcal{O}(F_1)}$. The superscript and the subscript represent the order of magnitude of the material flows within the block, and the set of labels of the units constituting the composite unit, respectively.

Figure 4 shows a pure recycle over N units with F_R being the recycle flow, and its equivalent representation

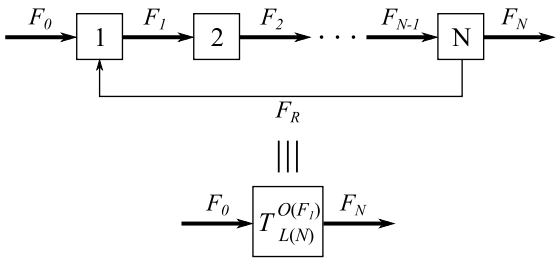

Fig. 3. Throughput and its equivalent composite unit

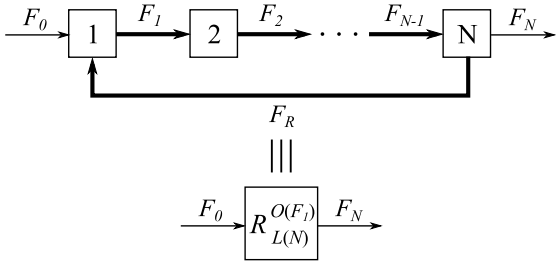

Fig. 4. Recycle and its equivalent composite unit

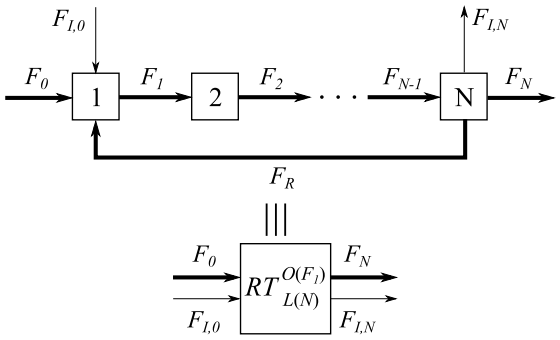

Fig. 5. Partial recycle/throughput and its equivalent composite unit

as a composite node $R^{\mathcal{O}(F_1)}_{L(N)}$. The same definitions of the superscript and the subscript are used.

Figure 5 shows a partial recycle/throughput over N units with the combination of a throughput and a recycle. A composite unit, which is the equivalent representation of this network, is a unit labeled $RT^{\mathcal{O}(F_1)}_{L(N)}$.

Note that, in the case of partial recycle/throughput, we need to identify the chemical species whose total holdup in the recycle loop will evolve in the slow time scale. Let us define two vectors of binary variables $\mathbf{r}$ and $\mathbf{t}$ as follows:

$$r_k = \begin{cases} 1, & \text{if any large internal flow contains } k\text{-th species} \\ 0, & \text{otherwise} \end{cases}$$

$$t_k = \begin{cases} 1, & \text{if any large external flow contains } k\text{-th species} \\ 0, & \text{otherwise} \end{cases}$$

If $r_k = t_k$, the material flow structure around the recycle loop for k-th species forms a large throughput, and the material balance variables for k-th species evolve in the fast time scale only. If $r_k \neq t_k$, the material flow structure around the recycle loop for k-th species forms a large recycle, and the total holdup of k-th species in the recycle loop evolves in the slow time scale, while the holdup of k-th species in individual units evolves in the fast time scale.

In what follows, we propose a graph-theoretic algorithm to identify basic building blocks and replace them with composite units, and to design a hierarchical control structure for complex material integrated process networks.

2.3 Graph-theoretic algorithm

Algorithm 1. *MaterialDynamicsAnalysis*$(\mathcal{G}, W)$

Sort W in descending order
for $i = 1$ to Size(W) **do**
  m = W[i]; $\mathcal{H}_m$ = *InducedSubgraph*($\mathcal{G}$, m)
  $\mathcal{T}(\tau_m)$ = nodes $\in \mathcal{H}_m$
  for each node N $\in \mathcal{H}_m$ **do**
    if N is a composite node **then**
      add $\sum N_i$ to $\mathcal{Y}(\tau_m)$
    else
      add N to $\mathcal{Y}(\tau_m)$
    end if
  end for
  $\mathcal{U}(\tau_m)$ = Edges in $\mathcal{H}_m$
  C = *SmallestElementaryCycle*($\mathcal{H}_m$)
  while C $\neq \phi$ **do**
    GraphReduce($\mathcal{G}$,C,m)
    GraphReduce ($\mathcal{H}$,C,m)
    C = *SmallestElementaryCycle*($\mathcal{H}$)
  end while
  for all node N $\in \mathcal{H}_m$ **do**
    if N is a composite node **then**
      [**r**, **t**]=*FindComp*
    end if
  end for
  if degree(N) = 0 for any node N $\in \mathcal{H}$ **then**
    Add τ_m to RecycleTimes
    Add N_i to PureRecycles
    All but 1 out of N_i should be controlled in this time scale
  end if
  if degree(N) $\neq$ 0 for all nodes N $\in \mathcal{H}$ **then**
    Clear RecycleTimes, PureRecycles
  end if
  for all node N $\in \mathcal{H}$ such that degree(N) $\neq$ 0 **do**
    if N is a composite node **then**
      if RC(N)=TC(N) **then**
        Remove N_i from PureRecycles
        Remove N from $\mathcal{G}$
      else
        Add τ_m to RecycleTimes
        Add N to PartialRecycles
      end if
    else
      Remove N from $\mathcal{G}$
    end if
  end for
end for
return $\mathcal{T}, \mathcal{Y}, \mathcal{U}$

Algorithm 1 outlines the procedure for simplifying a complex process flow graph and formulating a hierarchical control design by exploiting the multi-time scale dynamics. The inputs to the algorithm are the graph $\mathcal{G}$(N,E) and a

vector W of the various orders of magnitude exhibited by different material flows. The outputs of the algorithms are:

- $\mathcal{T}$, a set such that $\mathcal{T}(\tau_m)$ refers to the set of the material balance variables evolving in the time scale τ_m.
- $\mathcal{Y}$, a set such that $\mathcal{Y}(\tau_m)$ refers to the set of the material balance variables to be controlled in the time scale τ_m.
- $\mathcal{U}$, a set such that $\mathcal{U}(\tau_m)$ refers to the set of potential manipulated inputs (i.e. material flows) available in the time scale τ_m.

Since one seeks the evolution of the system for times $t = 0 \rightarrow \infty$, the algorithm begins with the largest order of magnitude material flows (corresponding to the fastest time scale) and proceeds to the smallest. For a given order of magnitude 'm', a subroutine *InducedSubgraph* extracts a subgraph '$\mathcal{H}_m$' from $\mathcal{G}$ such that all the edges in $\mathcal{H}_m$ have m as its maximum weight (i.e. the order of magnitude of the overall flow rate is m). As the dynamics of the total holdups as well as the species holdups of the nodes in $\mathcal{H}_m$ are affected by the material flows of the order m, they evolve in the time scale τ_m. Thus, all the nodes (essentially, the total holdups and the species holdups) in $\mathcal{H}_m$ are added to $\mathcal{T}(\tau_m)$. Also, all the edges in $\mathcal{H}_m$ are added to $\mathcal{U}(\tau_m)$.

The subroutine *SmallestElementaryCycle* identifies the smallest cycle in $\mathcal{H}_m$, which corresponds to a large recycle. Once a cycle $\mathcal{C}$ is found, the nodes in $\mathcal{C}$ are replaced by a composite node using the subroutine *GraphReduce*. The while loop is introduced to ensure that all the cycles in $\mathcal{H}_m$ are replaced by composite nodes (note that the while loop terminates if $\mathcal{C} = \phi$, where ϕ represents an empty set). Once the operation of the while loop is completed, $\mathcal{H}_m$ contains only composite recycles and/or throughputs. For each composite recycle node, the compositions of the recycle flows and the throughput flows, $\mathbf{r}$ and $\mathbf{t}$, respectively, are identified through the subroutine *FindComp*.

Then, for each composite recycle node, we identify the nature of it based on the degree (i.e. the number of edges connected to the node), $\mathbf{r}$, and $\mathbf{t}$, as discussed in the previous subsection.

The linear dependence/independence of quasi-steady state constraints plays a key role in model reduction within the framework of singular perturbations. Specifically, if the quasi-steady state constraints obtained from the time scale τ_m at a reduction step are linearly independent, all the material balance variables represented by the nodes in $\mathcal{H}_m$ evolve only in the time scale τ_m, while the dynamics in the time scale τ_m are accompanied by slower evolution in the subsequent time scales (e.g. τ_{m-1}) if such constraints are linearly dependent.

Note that the linear dependence/independence of quasi-steady state constraints can also be predicted from the graphs. Pure/partial recycles will result in linearly dependent quasi-steady state constraints, since there is no input/output of all (in the case of pure recycle) or some (in the case of partial recycle) chemical species for such recycles. Linearly independent quasi-steady state constraints will be obtained from pure throughputs. As the dynamics of pure throughputs evolve in a single time scale, all the pure throughputs are removed from $\mathcal{G}$.

Remark 1. Chemical reactions with rates of different orders of magnitude can also lead to a multi-time scale dynamics. If the characteristic times of the reactions are comparable with the time scales induced by different flowrates, then the chemical reactions can be included in the different subgraphs generated by the algorithm. Considering cases where different chemical reaction rates induce additional time scale multiplicity is beyond the scope of this paper.

3. CASE STUDY - HMF PRODUCTION PROCESS

3.1 Process description

Let us consider a process network proposed in Torres et al. (2010) to produce 5-hydroxymethylfurfural (HMF) from fructose. As shown in Figure 6, the process consists of a biphasic reactor coupled with an extractor and an evaporator. A solution containing fructose and catalyst

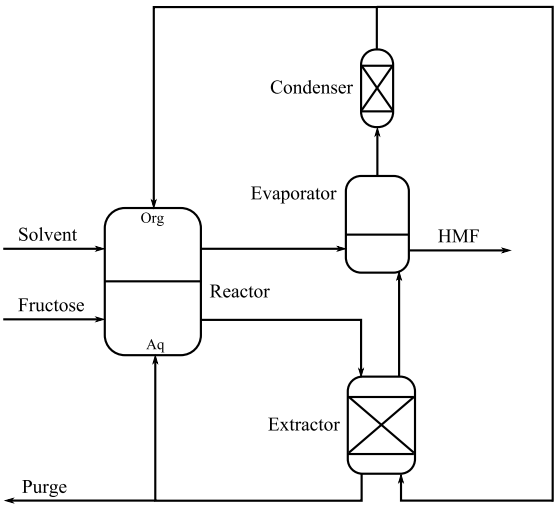

Fig. 6. Process flow diagram of the HMF production process

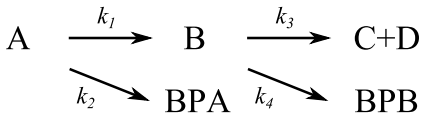

Fig. 7. Simplified reaction network of the HMF production process

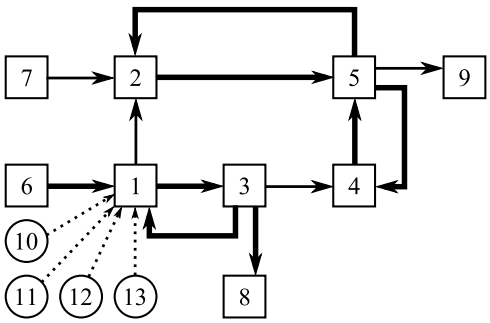

Fig. 8. Process flow graph of the HMF process

Normal nodes		Auxiliary nodes	
Node	Unit	Node	Unit
1	Reactor(aq)	6	Fructose feed
2	Reactor(org)	7	Solvent feed
3	Extractor(aq)	8	Purge
4	Extractor(org)	9	Product
5	Evaporator		
Reaction nodes			
Node	Reaction		
10	Fructose → HMF		
11	Fructose → BPA		
12	HMF → Levulinic acid + Formic acid		
13	HMF → BPB		

Table 2. Node list of the HMF process flow graph

Index	Species	Index	Species
1	Fructose	5	BPA
2	HMF	6	BPB
3	Levulinic acid	7	Water
4	Formic acid	8	Organic solvent

Table 3. Index list for the chemical species

Edge	Values	Edge	Values
1→2	(0,1,0,0,0,0,0,0)	5→4	(0,1,0,0,0,0,0,2)
1→3	(1,1,1,1,1,1,2,0)	5→9	(0,1,0,0,0,0,0,0)
2→5	(0,1,0,0,0,0,0,2)	6→1	(1,0,0,0,0,0,2,0)
3→1	(1,1,1,1,1,1,2,0)	7→2	(0,0,0,0,0,0,0,1)
3→4	(0,1,0,0,0,0,0,0)	10→1	(-1,1,0,0,0,0,3,0)
3→8	(1,1,1,1,1,1,2,0)	11→1	(-1,0,0,0,1,0,0,0)
4→5	(0,1,0,0,0,0,0,2)	12→1	(0,-1,1,1,0,0,-2,0)
5→2	(0,1,0,0,0,0,0,2)	13→1	(0,-1,0,0,0,1,0,0)

Table 4. Edge list of the HMF process flow graph

are fed to a continuously stirred biphasic tank reactor. Figure 7 shows a simplified kinetic model for this system. This model accounts for the losses of fructose (A) due to the formation of products other than HMF (B) lumping them under a single term (BPA), neglects the existence of intermediate products between fructose and HMF, considers levulinic (C) and formic acids (D) as the main HMF rehydration products and lumps the rest of the byproducts into a single term (BPB). The reaction takes place in the aqueous phase while the organic phase composed of 7:3 methyl iso-butylketone:2-butanol selectively extracts the HMF produced, thus minimizing its decomposition. The aqueous stream exiting the reactor is sent to a liquid-liquid extractor to recover the fraction of HMF that remains in it, and is then recycled back to the reactor. A purge stream is required to prevent the accumulation of byproducts in the reactor aqueous phase. The streams exiting the organic phase of the reactor and the extractor are sent to the evaporator, from where purified HMF is obtained as the product. The evaporated solvent is recycled back to the extractor and the reactor. A small amount of fresh solvent is also added to the organic phase of the reactor to maintain the solvent inventory in the system.

The presence of a purge stream and multiple recycle loops along with the segregation of material flows (as documented in Jogwar et al. (2012)) suggests that there would be a possibility for the network to exhibit multi-time scale material dynamics. In what follows, we apply

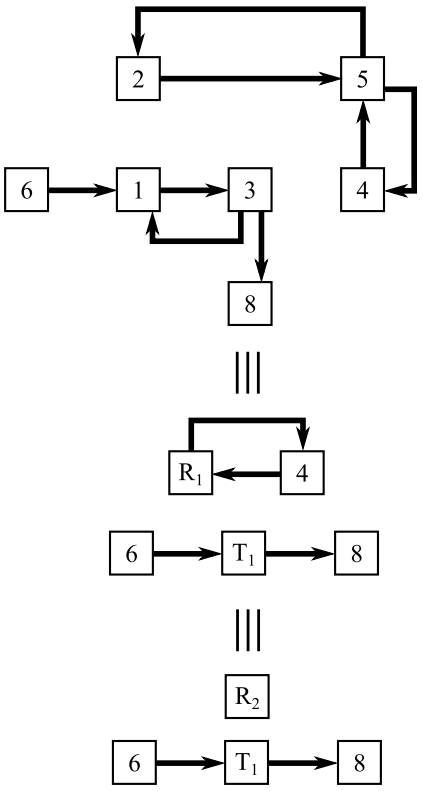

Fig. 9. Subgraph of the HMF process: fast time scale

State	Node				
	1	2	3	4	5
M	O	O	O	O	O
c_1	O		O		
c_2	O	O	O	O	O
c_3	O		O		
c_4	O		O		
c_5	O		O		
c_6	O		O		
c_7	O		O		
c_8		O		O	O

Table 5. Summary of the fast time scale dynamics of the HMF production process

the proposed graph-theoretic algorithm to this process network.

3.2 Graph-theoretic analysis

The process network shown in Figure 6 can be represented as a graph as shown in Figure 8. The node list of the graph is provided in Table 2. The indices for different chemical species presented in the network are summarized in Table 3. The edge weight information was taken from Jogwar et al. (2012), and summarized in Table 4. We apply the proposed graph-theoretic algorithm to this process network using information from Figure 8 and Table 4. The result on the graph reduction is shown in Figures 9 and 10.

Figure 9 shows the subgraph of the process flow graph with the large flows. The units evolving in the fast time scale are $\mathcal{T}(\tau) = \{1, 2, 3, 4, 5\}$. This subgraph contains two pure recycles (which are connected with each other) and one pure throughput, which can be simplified as composite

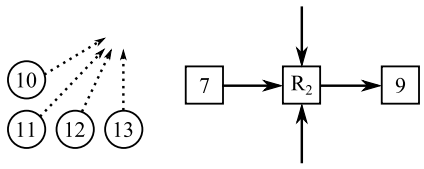

Fig. 10. Subgraph of the HMF process: slow time scale

State	Node				
	1	2	3	4	5
M		O		O	O
c_1					
c_2		O		O	O
c_3					
c_4					
c_5					
c_6					
c_7					
c_8		O		O	O

Table 6. Summary of the slow time scale dynamics of the HMF production process

nodes R_2 and T_1. As the dynamics of pure throughput blocks evolve only in this time scale, T_1 is removed from the original graph. The subgraph of the process flow graph for the slow time scale is shown in Figure 10. A subset of the units which evolve in this time scale are given by $\mathcal{T}(t) = \{R_2\}$. Note that this subgraph contains trivial edges arising due to the removal of T_1.

Based on the above result, this network is expected to exhibit two time scale material dynamics, and the material balance variables which evolve in the fast and slow time scales are summarized in Table 5 and Table 6, respectively. Note that this result matches the singular perturbation analysis provided in Jogwar et al. (2012).

Also, the controlled outputs and the potential manipulated inputs available in each time scale can be identified. In the fast time scale, the following set of the controlled outputs is identified: $\mathcal{Y}(\tau) = \{M_1, M_2, M_3, M_4, M_5, c_{1,1}, c_{2,1}, c_{3,1}, c_{4,1}, c_{5,1}, c_{6,1}, c_{7,1}, c_{2,2}, c_{8,2}, c_{1,3}, c_{2,3}, c_{3,3}, c_{4,3}, c_{5,3}, c_{6,3}, c_{7,3}, c_{2,4}, c_{8,4}, c_{2,5}, c_{8,5}\}$.

Note that, since R_2 is a pure recycle node, all but one variables in each of the following sets should be controlled:

$$\{M_2, M_4, M_5\}$$
$$\{c_{2,2}, c_{2,4}, c_{2,5}\}$$
$$\{c_{8,2}, c_{8,4}, c_{8,5}\}$$

Potential manipulated inputs in this time scale include: $\mathcal{U}(\tau) = \{F_{6-1}, F_{1-3}, F_{3-1}, F_{3-8}, F_{2-5}, F_{5-2}, F_{4-5}, F_{5-4}\}$.

In the slow time scale, the total holdup and the holdups of the species 2 and 8 of R_2 need to be controlled, i.e. $\mathcal{Y}(t) = \{M_{R_3}, c_{2,R_3}, c_{8,R_3}\}$. The following set of potential manipulated inputs is identified: $\mathcal{U}(t) = \{F_{7-R_2}, F_{R_2-9}\}$.

4. CONCLUSION

In this paper, we proposed a graph based approach to analyze complex material integrated process networks. First, a graph representation of a process network (a process flow graph) was proposed. Then, a graph-theoretic algorithm which can automatically generate information on the time scales exhibited by different units in the network, and the controlled outputs and the potential manipulated inputs available in each time scale. The application of the proposed framework was illustrated using a HMF production process network as an example. Future work will address the graph reduction of both the material and energy dynamics of integrated networks with segregation of material and energy flows.

REFERENCES

Baldea, M., Daoutidis, P., and Kumar, A. (2006). Dynamics and control of integrated networks with purge streams. *AIChE J.*, 52(4), 1460–1472.

Friedler, F., Tarjan, K., Huang, Y., and Fan, L. (1992). Graph-theoretic approach to process synthesis: axioms and theorems. *Chem. Eng. Sci.*, 47(8), 1973–1988.

Heo, S., Jogwar, S., Rangarajan, S., and Daoutidis, P. (2012). Graph reduction for hierarchical control of energy integrated process networks. In *Decision and Control (CDC), 2012 IEEE 51st Annual Conference on*, 6388–6393. IEEE.

Heo, S., Rangarajan, S., Daoutidis, P., and Jogwar, S. (2014). Graph reduction of complex energy-integrated networks: Process systems applications. *AIChE J.*, 60(3), 995–1012.

Hudon, N. and Bao, J. (2012). Dissipativity-based decentralized control of interconnected nonlinear chemical processes. *Comput. Chem. Eng.*, 45, 84–101.

Jogwar, S., Baldea, M., and Daoutidis, P. (2009). Dynamics and control of process networks with large energy recycle. *Ind. Eng. Chem. Res.*, 48(13), 6087–6097.

Jogwar, S., Rangarajan, S., and Daoutidis, P. (2011). Multi-time scale dynamics in energy-integrated networks: A graph theoretic analysis. In *IFAC World Congress*, volume 18, 6085–6090.

Jogwar, S., Torres, A., and Daoutidis, P. (2012). Networks with large solvent recycle: Dynamics, hierarchical control, and a biorefinery application. *AIChE J.*, 58(6), 1764–1777.

Kumar, A. and Daoutidis, P. (2002). Nonlinear dynamics and control of process systems with recycle. *J. Process Contr.*, 12(4), 475–484.

Liu, J., Muñoz de la Peña, D., and Christofides, P. (2009). Distributed model predictive control of nonlinear process systems. *AIChE J.*, 55(5), 1171–1184.

Mhaskar, P., Gani, A., McFall, C., Christofides, P., and Davis, J. (2007). Fault-tolerant control of nonlinear process systems subject to sensor faults. *AIChE J.*, 53(3), 654–668.

Rawlings, J. and Stewart, B. (2008). Coordinating multiple optimization-based controllers: New opportunities and challenges. *J. Process Contr.*, 18(9), 839–845.

Sun, Y. and El-Farra, N. (2008). Quasi-decentralized model-based networked control of process systems. *Comput. Chem. Eng.*, 32(9), 2016–2029.

Torres, A., Daoutidis, P., and Tsapatsis, M. (2010). Continuous production of 5-hydroxymethylfurfural from fructose: a design case study. *Energy Environ. Sci.*, 3(10), 1560–1572.

Ydstie, B. (2002). Passivity based control via the second law. *Comput. Chem. Eng.*, 26(7), 1037–1048.